ADVANCED PHOTONICS RESEARCH
Open Access
www.adpr-journal.com

Self-Reporting Hydrogel Sensors Based on Surface Instability-Induced Optical Scattering

*Imri Frenkel, Mutian Hua, Yousif Alsaid, and Ximin He**

Interest regarding the development of hydrogel sensors continues to grow due to the associated high sensitivity, fast response, low fabrication cost, and versatile application when responding to an analyte. The strategies for transducing these responses range from electrochemical to optical, often utilizing characterization equipment to measure the minute changes in the material. However, the costly nature of such equipment counteracts the original advantages of utilizing a hydrogel-based sensor, rendering the overall system slow and inaccessible for many. Therefore, hydrogel sensors capable of self-reporting values to the naked eye are needed. Here, a new light-scattering-based transduction method is explored—indiscriminately visible to the naked eye. By engineering the surface instability behavior of a hydrogel film, an exemplary design is developed using an anionic, pH-responsive poly(acrylamide-*co*-acrylic acid) hydrogel to self-report the pH via subsequent buckling (i.e., its scattering of light). By modeling the behavior based on three system parameters (critical concentration, critical swelling ratio, and modulus), a general design model is produced to guide practical implementations of this instability-induced scattering (IIS) sensor system. The viability of the IIS design model is exemplified through a proof-of-concept application to sensing urea, illustrating the modular and adaptable design of the presented transduction method.

1. Introduction

Water pollution,[1,2] environmental toxins,[3,4] hazardous substances,[5,6] the rise of synthetic recreational drug alternatives like fentanyl,[7–9] chemical warfare agents,[10,11] tumor-specific molecular indicators, insulin levels in diabetics, glucose levels in hypoglycemics, there is certainly no shortage of unique molecules and chemicals that necessitate a quick, sensitive, and in situ method of sensing their presence, especially in aqueous and bodily environments. To date, there exists a multiplicity of methods[4,6,12–14] capable of sensing significant analytes like those aforementioned and more, be it chromatography, mass spectrometry, electrochemistry, absorption spectroscopy, or IR and Raman spectroscopies, for example.

Many contemporary works have looked to hydrogels or hydrogel actuated systems as leading candidates to increase sensitivity due to the large volume change of hydrogels upon stimulation.[15–18] These polymer networks have shown great promise, as they are in general highly tunable and relatively cheap to produce, while offering various avenues of transduction. The fundamental mechanism of stimuli–responsive hydrogels is well understood, as a multitude of published literature documents these flexible polymer matrices' abilities to contract or expand in response to analytes in the environment. The hydrogel may be chemically functionalized and adapted to respond to an analyte of one's choice and thus set the gel's response to the desired outcome (based on Flory–Huggins' theory of hydrogel volume phase transitions [VPT]).[15,19–22] Consequently, there exists a multitude of methods to communicate the presence of this swelling phenomena and the degree to which it occurs (i.e., transduce). These methods of transduction can be organized under three main groups: electrochemical (e.g., measuring changes in current, voltage, or resistance through the gel),[4,9,23] mass based (e.g., measuring changes in weight or normal forces of the gel), and optical (e.g., measuring changes in absorbance, fluorescence, diffraction, or transmission of the gel),[11,24,25] in that the routes of transduction of each said group measure changes in properties corresponding to each said group.

Though the hydrogel sensor itself serves as a low-cost and broadly applicable substitute for a similarly responsive sensor, the transduction of information is not immediately apparent, depending on the avenue chosen for transduction. Most of the aforementioned techniques rely heavily on instruments for reading the output; thus many, if not all, of these methods suffer from some combination of expensive or difficult-to-use equipment and restrictive and time-consuming sample preparation. The reliance on finicky, specific, and sensitive digital equipment to accurately relay the hydrogel's volumetric changes to readable information in many ways counteracts the initial cost advantage and has prevented the application of hydrogel sensors to instances requiring on-site detection. This can be particularly the case

I. Frenkel, M. Hua, Y. Alsaid, Prof. X. He
Department of Materials Science and Engineering
University of California
Los Angeles, CA 90095, USA
E-mail: ximinhe@ucla.edu

The ORCID identification number(s) for the author(s) of this article can be found under https://doi.org/10.1002/adpr.202100058.

DOI: 10.1002/adpr.202100058

for mass-based and electrochemical transduction methods, which rely on carefully monitoring minute changes in magnetoelastic or potentiometric properties, respectively. Hence, a self-reporting hydrogel sensor that integrates both sensing and signal transduction into a readable output would be advantageous for developing a low-cost and user-friendly sensor system.

Optical transduction pathways have shown great promise for producing naked-eye sensors that do not involve, or otherwise minimally involve, the use of instruments for obtaining readable results, be it changes in color via absorbance or light intensity via emission as drastic changes in thickness of the hydrogel are instantly perceived.[26–30] However, reference charts/tables are still required for these methods and external equipment may be necessary to communicate very minute changes in color, as the output signals from the hydrogel sensors are linearly distributed in the form of continuous color changes.

Recently, studies on hydrogel surface instability have shown a viable pathway for enabling hydrogel sensors with digitized, self-reporting capabilities.[31,32] The stimuli-driven expansion of the polymer network of a hydrogel can drive the generation of surface instabilities on the gels when the gels' expansion is inhibited by physical confinement. As a result, the spontaneous generation of these instabilities at distinct critical values of swelling responses visibly disrupts the transparency of the hydrogel by scattering light. Specifically, the onset of these surface instabilities is thresholded as the transformation is abrupt rather than linear, rendering this method an all-or-nothing, discrete manifestation.

Here, this surface instability phenomenon is taken advantage of in the creation of a new hydrogel-based sensor that relays analyte concentration into true naked-eye readable signals through optical scattering, referred to as an instability-induced scattering sensor (IIS sensor). Through tuning of the hydrogel mechanics and its sensitivity to a chosen analyte, in conjunction with the thresholding characteristic of said surface instabilities, the IIS sensors were engineered to indicate the absolute concentration of the analyte without the aid of external references or equipment, thus exhibiting consistent, self-reporting capabilities. To demonstrate the underlying mechanism and versatility of this system, an anionic, urea-sensing system was synthesized and its behavior modeled for extrapolation beyond this work. The instability-based hydrogel sensor provided herein illustrates a proof of concept that may be universally applied to any past or future hydrogel functionalization which utilizes VPT and provides an avenue for others' hydrogel systems to be applied practically, whereby untrained users may easily rely on such sensors to quickly and accurately communicate the presence of specific vital or toxic molecules in a given aqueous environment, be it insulin levels in blood or heavy metals in water supplies.

2. Results and Discussion

2.1. Material and System Design

Despite current optically transducing hydrogel sensors, which rely on changes in color, demonstrating promising performance in their own right, certain persisting limitations associated with such devices served as the primary motivation for the development of the IIS system fabricated herein, especially as it pertains to indiscriminate, inherent, naked-eye readability. To reliably identify a gel's color shift of 70 nm, or sometimes even much more, necessitates assistance from an external digital readout, once again negating the very advantages these hydrogel sensors seek to address. Physically, the sensing performance of cone cells in a human eye is variable, fluctuating in sensitivity up to 10 nm or more depending on the incident light's wavelength,[33]—yet even this precision can be elusive to achieve as it is psychologically difficult to realize. Works investigating the evolution of naming schemes across languages illustrated the subjective nature of recognizing color contrasts of smaller step size despite being no more or less physically capable of differentiating colors.[24] This is further evident when comparing the variance of individuals' ability to perceive color changes across different inherent genetic make-ups and a plethora of yet to be fully defined nongenetic influences.[34–38] Furthermore, the perceived shade, tint, tone, and even overall hue, may be manipulated by the contextual lighting.[39] These variances are all observed in young, healthy individuals. Those with color vision impairments are of course greatly more deviant, which raises questions regarding the accessibility of such color-based transduction methods. All this is to say that despite the rightfully endowed advantages of current optical transduction methods, to date, these methods remain imperfect—especially in their ability to be used indiscriminately, in situ, and by any layman user without the aid of external equipment or reference.

Figure 1a shows the synthesis and working principle of the aforementioned IIS sensor. Briefly, hydrogel films with thickness of ≈140 μm were fabricated on double-bond-grafted rectangular glass slides via molding and subsequent UV-initiated free-radical polymerization. Compositions of the gels were confirmed by Fourier-transform infrared spectroscopy (FTIR) (Figure S1, Supporting Information). The hydrogel film was transparent in the deswelled state. In the presence of stimuli that induce swelling of the hydrogel, the hydrogel film formed surface instabilities that strongly scattered light, resulting in a blurred translucency when viewing through the hydrogel (Figure 1b and Figure S2, Supporting Information).

The transduction of analyte concentration to optical signal is shown in Figure 1c and operates through the following underlying mechanism. As chemically attractive analytes diffuse through the deswelled gel, freely coiled portions of the network chain are driven to uncoil to maximize surface interaction with the surrounding charged environment. This outward osmotic pressure (yellow arrows) in turn results in the observed volume expansion under typical circumstances; however, this is prohibited by the physical confinement of the gel as it shares covalent bonds with the functionalized glass substrate along their interface. Given only a thin layer of gel, there is limited driving force and geometric capability to expand in height away from the substrate, so the confinement can be represented horizontally along the glass−gel interface and in part vertically along the gel−air interface and orthogonal to the substrate—as illustrated by the gray corner marks. This bilateral confinement produces normal forces that compress the gel inward and tangent the substrate (red arrows) through the gel's surface. Consequently, stress concentrations form along the gel's surface. Ultimately, it is the steady growth of these stress concentrations that drives the rapid proliferation

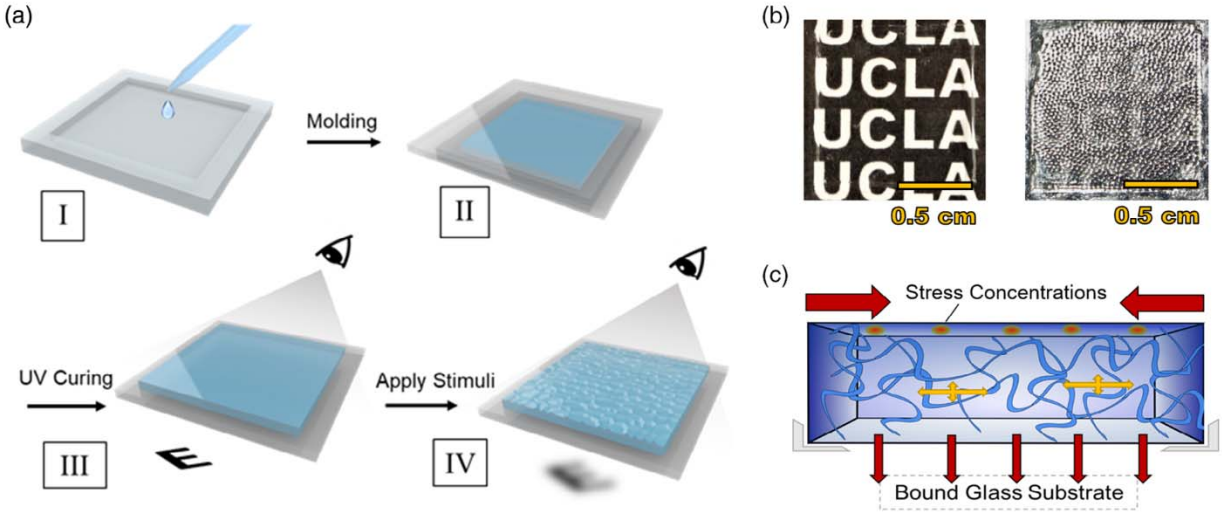

Figure 1. Fabrication and working principle. a) Fabrication of the glass-bonded hydrogel film. (i) Dissolving of monomers, crosslinkers, and initiators and then filling PDMS mold (depth 140 µm) with 160 mL of solution. (ii) Covering with functionalized glass slide. (iii) UV-initiated polymerization for 60 s while on cooling stage; the transparent and smooth gel adhered to the substrate is removed from the mold. (iv) Upon sufficient stimulation, gel attempts to swell, but due to its confinement, surface instabilities form to relieve the building internal stress. b) Photograph of an unwrinkled gel (left) and wrinkled gel, resulting from exposure to stimulation (analyte concentration) beyond its associated critical threshold value for the onset of surface instability (right). Scale bar located at the bottom right of the image equates to ≈0.5 cm. c) Illustration of the mechanism driving the spontaneous surface instability (i.e., wrinkle) phenomena within the hydrogel network (blue).

of instability formations once the energy associated with relieving this strain is greater than the energy thresholds associated with internal mechanical performance (i.e., modulus) and surface energy interactions.

2.2. Exemplary pH Sensor Performance

In producing the practical experimental setup of this work's focus, first, the critical stimuli values were obtained for various recipes ranging in their ratio of monomer-to-monomer content. Here, the basic stimulus from which the proposed design is generalized is pH. Knowing the pH value required to insight buckling indicates the threshold required of any acidification/alkalization of the environment via analyte oxidation, like the enzymatic reactions of urea or glucose, for example.

The exemplifying anionic sensor provided in this work consisted of poly(acrylamide-*co*-acrylic acid) hydrogel and was used to fabricate the IIS sensors, as previously shown in Figure 1a. By tuning the monomer concentration of the precursor used to fabricate the hydrogel, IIS sensors with various instability-forming thresholds were obtained, meaning that these IIS sensors form such surface instabilities and appear wrinkled at or above different critical pH values depending on the corresponding hydrogel constitutions. Each recipe is designated by its associated percent monomer content of acrylamide (X%) and acrylic acid (Y%) by weight relative to the total mass of precursor solution (i.e., X%−Y%, respectively).

In **Figure 2**a, the on−off buckling response of IIS sensors with different critical buckling thresholds was demonstrated, where each sensor portrayed an increasingly higher critical pH value (pH_c) and thus possessed an increased threshold to instability formation across recipes from top to bottom row of Figure 2a. The numbers behind each sensor voxel indicated the pH value of the solution applied to the sensors at that given position and the clear-to-blurry-wrinkled transformation observed by the naked eye indicated the characteristic instability formation. Images taken of the gels in environments of increasingly alkaline pH portrayed the critical response value for each gel. IIS sensors with increased monomer content possessed an increased critical threshold, and this tunability of the gels' pH_c at which buckling is induced is further illustrated and quantified through consequential changes in transmittance, as shown in Figure 2b, as well. Though more apparent through naked-eye observation, the notable change in transmittance, and the pH value at which it occurs, displayed the directly proportional relationship between the gel's monomer content and pH_c. Thus, one IIS sensor with a known threshold value determined by the hydrogel constitution could indicate the magnitude of the pH of an unknown solution relative to the built-in threshold value. That is to say, if an IIS sensor has not yet buckled, it is known that the associated critical analyte concentration has not yet been reached, but when IIS appears to the observer, it is known that the concentration is equal to or greater than its threshold. Thus, using an array of IIS sensors with different critical thresholds can yield an accurate reading of the analyte value, in this case pH, of an unknown solution, just as observed, looking down each column in Figure 2a, where the pH values are equivalent but sensor recipes differ.

Given that the wrinkled state arises as a consequence of the hydrogel's swelling response to analyte concentration, the IIS performance of each gel can be described by its swelling behavior, as well. By measuring the ratio of each unhindered hydrogel's additional top−down area after exposure to a given environment free of any substrate relative to its initial top−down area in its deswelled state, a swelling ratio value can be correlated

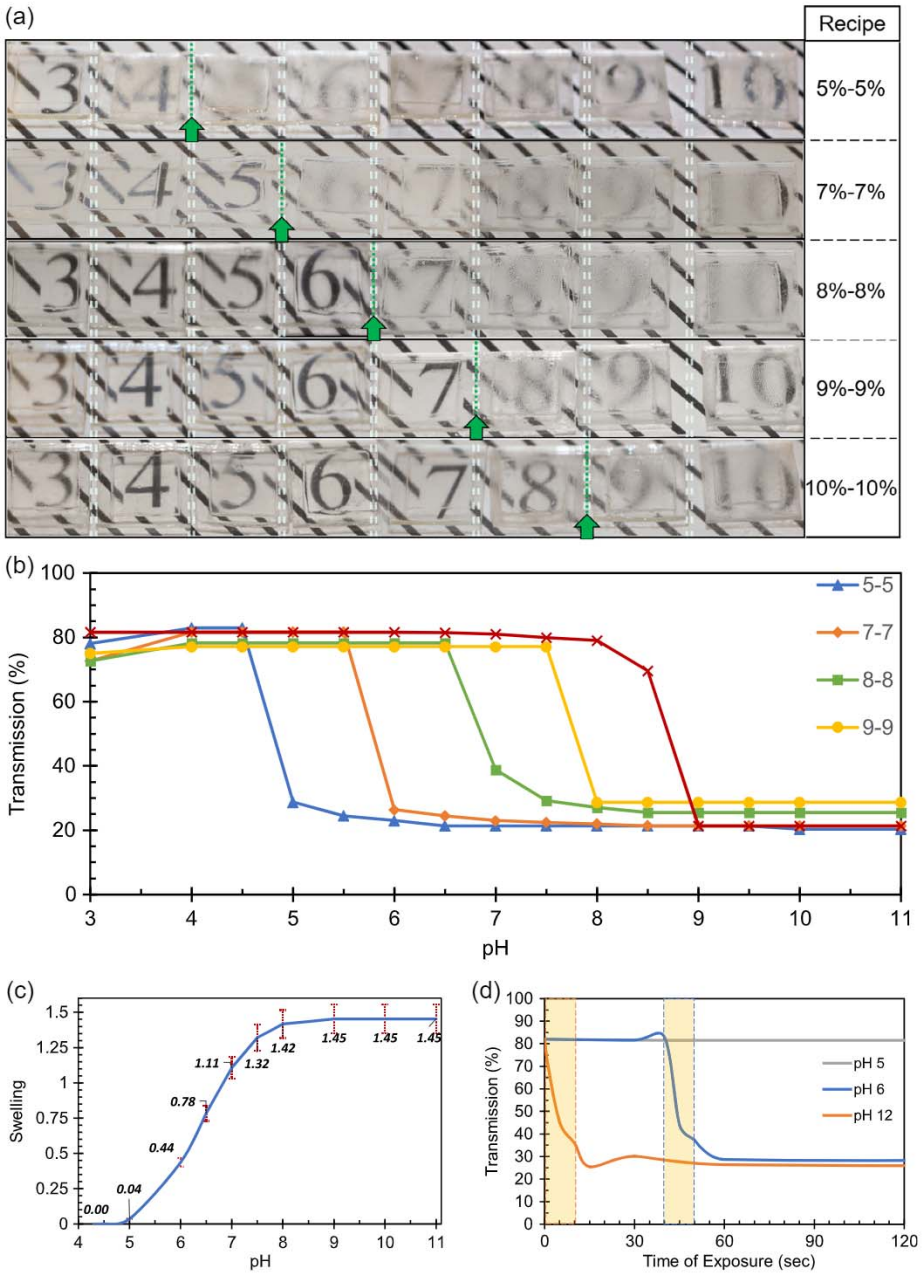

Figure 2. Mechanistic behavior. a) pH 3–10, showing critical pH at pH = 5, 6, 7, 8, and 9, respectively, for anionic gels containing increasing acrylamide–acrylic acid contents by weight from 5%–5% (top) to 10%–10% (bottom). b) Transmittance curves of recipes imaged in (a), illustrating the critical pH threshold at which each gel transforms from transparent to buckled, discretely and increasing with increasing elastic modulus. c) Swelling behavior of anionic gel (7%–7% acrylamide–acrylic acid, elastic modulus [E] = 69 kPa) relative to the gel's resting volume dictated by acrylic acid's pK_a of 4.3. Error bars correspond to an average normalized standard deviation of ≈7%. d) Response time and transmittance of 7%–7% anionic gel at pH of 6 (blue) and pH of 12 (orange) following increasing duration of exposure to the analyte concentration via submersion in solution. These are compared with the transmittance of the yet-to-be buckled gel exposed to a pH of 5 (gray), below its critical threshold pH of 6. Yellow–orange regions delineate the 10 s transition periods of the gels as they transform from the smooth, transparent state to wrinkled, blurry state. Transmission data displayed for select pH levels with concern for visual clarity and clear comprehension of the window of time corresponding to the IIS sensor's time to transform at the lowest bound of its sensitivity, pH_c (pH = 6), and upper bound of typical usage (pH = 12). A pH of 5 corresponds to analyte concentration just below pH_c and serves as a baseline reference to control for change due to arbitrary submersion in a solution. Full transmission data provided in Figure S4, Supporting Information.

with each IIS sensor's pH_c and can ultimately prove an indirect measure for the internal stress within the confined hydrogel. Figure 2c shows an example of the relationship between swelling ratio and pH, using a 7%–7% recipe (acrylamide acrylic acid, respectively), indicating the corresponding IIS sensor that possessed a pH_c of 6 (Figure 2a,b) and possessed a critical swelling

ratio of ≈1.11. This is consistent with the general swelling behavior observed of such anionic gels (Figure S3, Supporting Information) as IIS sensors comprising a higher polymer content possessed greater critical swelling ratios directly proportional to their higher pH_c.

Though the visual response is apparent, the hydrogels' wrinkle transduction was quantified by way of measuring changes in the visible light transmitted through the gel over time while continuously exposed to a given pH environment. In addition to demonstrating the consistency of the light-scattering effect of the critically buckled hydrogel, the response time and its discrete on−off switch nature was portrayed, as all hydrogels examined began buckling after no more than 40 s and transitioned to the instability formation in less than a 10 s window (Figure 2d and Figure S4, Supporting Information). This behavior is consistent with gels of different recipes with different moduli (Figure S5, Supporting Information). Figure 2d shows this window of the IIS sensor's time to transform at both the lowest bound of its sensitivity (i.e., its critical pH_c of pH = 6) and what can be considered as a practical upper bound for commonly incurred alkalinity (pH = 12). The specific comparison between the extremities of the IIS's sensing range exemplifies the unchanging nature of the 10 s window that is the time to transform across its operational range. This is observed readily when comparing the sensor's transmittance following exposure with analyte concentrations below its pH_c (pH = 5 for the 7%−7% gel in Figure 2d and likewise a pH of 8 in Figure S4, Supporting Information, for a 10%−10% gel), given that the transmittance, and so observed transparency, remains by and large unchanged. In addition, this further confirms the apparent distinction between the gel's deswelled and wrinkled state and that the IIS formations do not occur at any arbitrary pH value given enough exposure time. It is clear, the transition is essentially discontinuous and, for all intents and purposes, instant—in terms of the practical, on-site, one-time testing applications this type of system might find use in.

In addition, it was noted that the time of exposure necessary to initiate IIS formations was inversely related to the distance the pH of the environment was from the pH_c associated with a given recipe (Figure S4e and S4d, Supporting Information). This indicated that the driving force for IIS formation is not simply the concentration of analyte in the environment; rather, it is dependent on the difference between environmental analyte concentration and the theoretical pH_c, which falls in line with the operational theory of this type of IIS transduction mechanism discussed thus far. Quantifying the progression of this relationship as a discrete mathematical relationship is not within the scope here in this work; however, it proves to be a promising topic of exploration in future studies looking to produce an IIS-based actuator with adaptable response(s) dependent on the time to initiate transformation.

2.3. Universal Design Model and Threshold Values

To expand the applicability of the exemplary setup and refine the sensitivity of the IIS sensor, we aimed to establish quantitative correlations between the onset of surface instabilities and measurable material properties in the entire variable space. Zhao and coworkers[32] demonstrated the predictability of this wrinkling phenomena by characterizing the rise of these instabilities on a hydrogel film adhered and confined to another hydrogel bulk based on three parameters: modulus ratio, adhesion energy, and mismatch strain (as an effect of each gel swelling independently) between the film and the bulk. Thus, a universal model inspired by the three axes of Zhao's model was created, serving as a design map for implementing the IIS sensor system universally to VPT-based hydrogel sensors and actuator.

It is important, however, to note the distinctions between past approaches through simulation and the practical approach seen in this work. Namely, the modulus of the glass substrate is orders of magnitude higher than that of the hydrogel and remains constant in all cases; therefore, the model may reliably communicate the behavior solely based on changes in the hydrogel's elastic modulus rather than the ratio between the two. In addition, the swelling responses are relatively weak compared with the adhesion achieved here, so the limitations of the swelling response with regard to delamination were not explored. Furthermore, past publications were preoccupied with the strain mismatch of the system; however, as the glass in this system is orders of magnitude more rigid than the gels to which they adhere to and are otherwise unaffected by changes in the environment, the strain mismatch can be simplified to solely the strain experienced by the hydrogel film itself. Moreover, the swelling incurred by the gel is a direct product of the internal strain in the gel generated by the attractive ionic and Van der Waals forces corresponding to the presence of a given analyte of interest. Thus, in the design model proposed here, a nonetheless insightful correlation, if not only more practical and intuitive, is ultimately provided via the relationship between swelling ratio, stimulant concentration, and modulus.

With the elastic moduli of each gel recipe acquired, a final "master model" was achieved (**Figure 3**). The correlation of each IIS sensor's elastic modulus to its threshold values elucidated the directly proportional interrelation between all three system parameters, especially as it pertains to the codependence of the critical threshold values (swelling ratio and pH_c) with the system's elastic modulus. That is, through the precise tuning of modulus by elementary alterations to polymer content within a hydrogel, an IIS sensor can be fabricated for any specific sensitivity within a vast range. This fundamental mechanism and design principle may be adapted universally to any VPT hydrogel system, beyond pH-sensitive gels, by consociating the system's modulus and the swelling response needed to observe IIS. Moreover, if the system utilizes an underlying oxidation reaction which creates pH-altering products, one may directly see the response value required—with respect to the environment and hydrogel itself—on the guiding model provided here.

2.4. Specific Analyte Detection

To demonstrate how this optical scattering transduction mode, IIS, may be used as a template for future and past works alike, a simple adaptation to sensing the presence of urea was explored. By introducing urease into the monomer solution, the significantly larger protein becomes partially entangled in the polymer network during polymerization—physically confined to the pores of the structure (Figure S6, Supporting Information). This

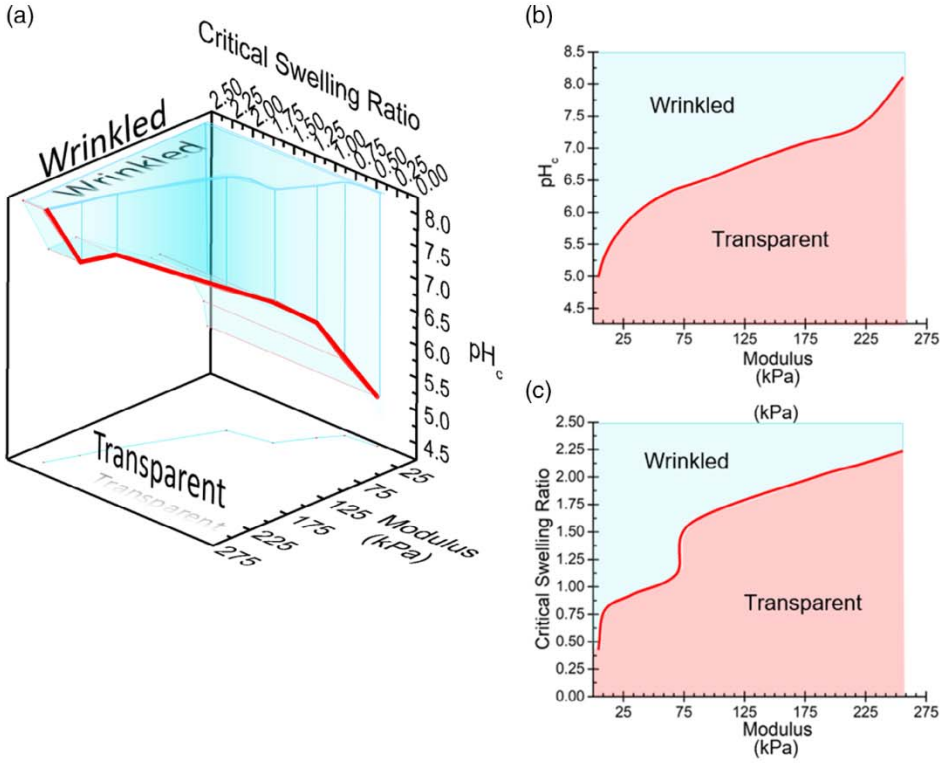

Figure 3. Guiding model's summative model a) of template pH-sensitive gel's swelling performance based on the interdependence of the gel's elastic modulus on its critical threshold operating parameters. b) Critical pH accurate to 0.5 pH. c) Critical swelling ratio at which point IIS occurs—i.e., wrinkles form.

enzymatic integration into the gel adds sensitivity to the specific enzyme's reaction products to the hydrogel sensor (in this case urea). This is useful here, whereby the reaction products possess different dissociation constants relative to the analyte in the environment solution, consequently altering the pH of the local environment within the gel. As specificity of sensing can be a priority in some applications, any specific enzyme may be easily incorporated as demonstrated (**Figure 4**a) to produce a gel specifically sensitive to the enzyme's complementary analyte. It is also possible to incorporate nonspecific enzymes if broader sensing capabilities are desired, as well. For nonenzymatically oxidized analytes, different recipe inclusions would be necessary dependent on the specific system's application (i.e., what it will sense), but similar specificity within the gel would be achieved. Regardless of inclusion, the same methodology and design principles demonstrated in this work may be followed—hence the universal applicability of this mechanistic template. Here, it is shown how the performance of the anionic gel can be modeled for the inclusion of urease, cross-referenced to the fundamental pH performance of the backbone network, and produce a final gel of desired sensitivity and responsiveness based on the gel's modulus.

After consulting the literature[40,41] and confirming experimentally, it was found that the maximum pH achievable through the urease reaction was approximately of pH 8.5. This guided the design window to matching a gel's swelling ratio in response to urea to that of a gel's swelling ratio in response to pH, as previously modeled. Thus, the same anionic gel recipes ranging from 10% to 4% acrylamide and acrylic acid content each were reproduced with inclusions of urease in amounts ranging from 0.1% by weight to 1% by weight, and their performances in response to urea were modeled and compared. To isolate recipes whose moduli dictated that their critical buckling stimuli were too large to be considered for the urea-sensitive gel ($pH_c > 8.5$), the gels' responses were modeled against a saturated solution of urea in water ($\geq$95% 1,079 g urea ml^{-1} at 20 °C),[42] to provide the maximum stimulation possible, and so, include the lowest sensitive gel possible at the expected ambient operating conditions. Figure 4b shows the urea response of a 7%−7% acrylamide−acrylic acid gel with the inclusion of urease over the said range. An initial peak in swelling response is observed at around 0.2–0.25% urease content by weight but subsequently begins to dip in performance. This occurred due to the urease's effect on the host network's modulus, as its entanglement effectively acts as a crosslinker that limits the hydrogel's ability to expand. Across recipes, decreases were observed in the range of 0.3–0.6% as the increases in modulus resulting from increased urease content outpaced the increases in swelling force produced by the increasing urease content. Beyond 0.6%, increases are again observed as the relationship inverts, until peaking at ≈0.9% where another fall-off in performance is observed. This second, lasting decrease results from the solubility issues observed for urease concentrations above 1% in the hydrogels and is detrimental to the hydrogel's ability to expand and swell. This relationship was observed in the swelling behavior of other recipes as well (Figure S7, Supporting Information), though this did not

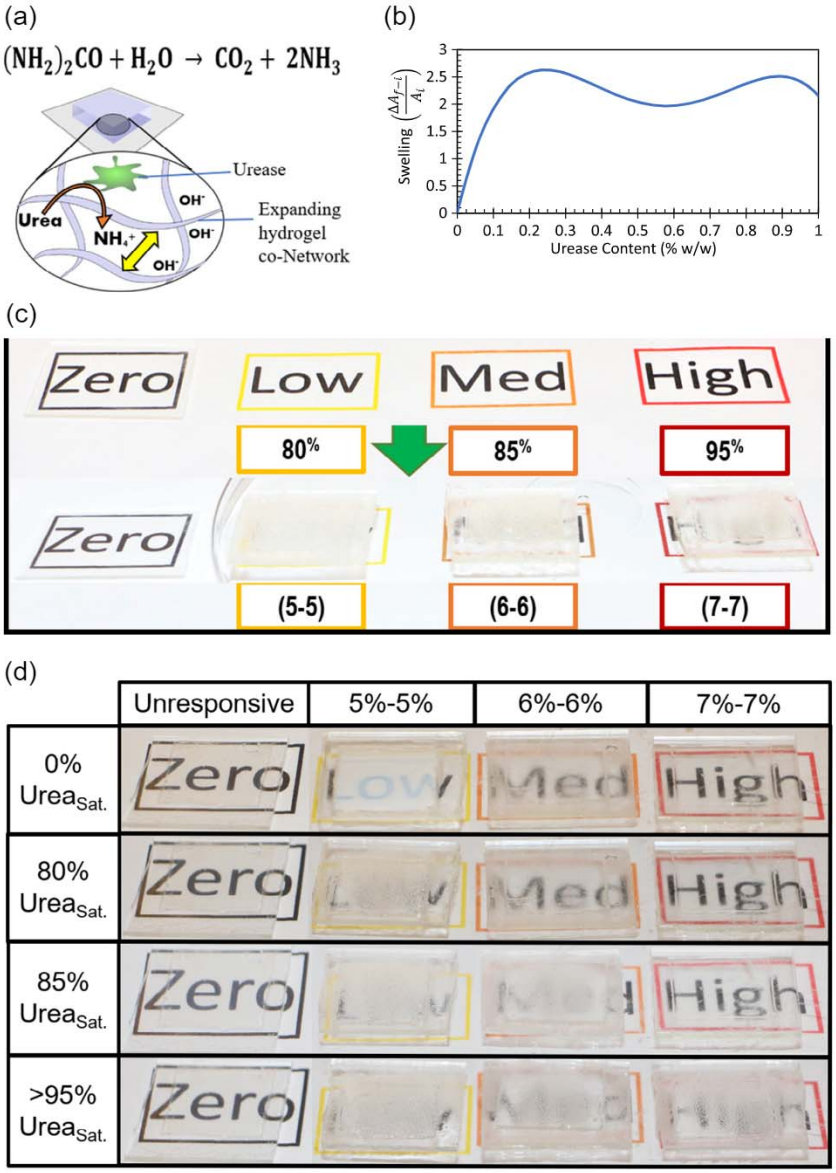

Figure 4. Urea detection performance. a) Enzymatically catalyzed oxidation of urea ($pK_a = 0.1$) by urease to produce ammonium ($pK_a = 37$) alkalizing the local water-rich environment within the gel. b) Measured swelling of gels containing varying amounts of urease incorporated into pH-responsive gels of 7%−7% acrylamide−acrylic acid content and submerged in a saturated solution (>95% solubility) of urea and water (1.01 g urea g^{-1} water or 95% of 1074 g L^{-1}). c) Three anionic gel recipes containing 0.2% urease by weight, whereby the 5%−5% acrylamide−acrylic acid gel (yellow), 6%−6% acrylamide−acrylic acid gel (orange), and the 7%−7% gel (red) have buckled after immersion in urea solutions corresponding to their, respective, minimum concentration sensitivities (859 g L^{-1} [80% saturation], 912.9 g L^{-1} [85% saturation], and ≈1074 g L^{-1} [>95% saturation], respectively), illustrating the tunable control of the optical-scattering transduction method via alterations to modulus. d) Demonstration of practical application as a sensor array, where a single set of gels was exposed to environments of varying concentrations of urea, from 0% to >95% saturation. The right-most IIS sensor, or least-sensitive IIS sensor, which has buckled, indicates the minimum concentration of urea possible within the solution it was exposed tp.

affect the discrete and rapid nature of the IIS transformation (Figure S8, Supporting Information). Thus, recipes containing urease in amounts greater than 1% by weight were not further examined. Ultimately, urea-responsive gels' swelling responses were measured at quantities of 0.2% urease by weight.

Given this behavior, a handful of gels were selected on the basis of their swelling ratio data at 0.2% urease exceeding their corresponding swelling ratio data for pH of 8.5. Three such recipes are shown in Figure 4c,d, displaying a buckled state following exposure to urea at their respective minimum critical concentration sensitivities, below which no buckling was observed. While the 7%−7% gel only responded to concentrations of urea greater than 95% saturation, 6%−6% gels could sense as low as 85% saturation and 5%−5% gels as low as 80% saturation, paralleling the variable performance observed in the purely pH-responsive gels studied prior. The tunable buckling response

of these gels based on the extrapolation of their responses to concentrations of urea demonstrated the potential effectiveness of such a system in an array (Figure 4d) and succeeded in illustrating the proof of applicability of this design process and for the instability-induced optical scattering-based method of transduction as a whole.

3. Conclusion

This work explored the behavior of instability formations on the surface of confined hydrogel as a means to transduce the presence of analytes in the surrounding environment due to the optical-scattering, and so visually apparent, nature of the resultant features. By modeling the buckling criteria via three main properties (stimulant concentration, swelling ratio, and modulus), a general model was produced from which the system may be applied to practical sensing applications. Adapting the model for use in a urea sensor exemplified the novel transduction system's versatility and proof of concept, and in doing so, the entirety of the novel design process was demonstrated as well. Hence, the model may be tailored to past and future hydrogel sensors alike, whereas the design process utilizing this type of optical-scattering transduction may be repurposed for more complex reaction response mechanisms in the future—hence the universal applicability of this mechanistic template.

Despite the success of this demonstration in explicating the versatility and proof of concept of this system and its methodology, some improvements may still be made in subsequent work. Namely, more complex systems will be the focus of future work, especially with regard to applying this transduction system to novel fentanyl sensors and chemical warfare agent sensors, as next steps in bringing this system to the real-world situations that demand it. Several potentially insightful avenues fell out of the scope of this work, in particular, the quantification of the exposure time to initiate transformation and exploring creative actuation designs by grouping sensor voxels in a stacked array or 2D matrix, for example. In addition, a more specific exploration of applications which demand low-adhesive substrates, but high-responsive gels, may be the subject of work more focused on the practical limitations of this transduction system relative to adhesion and delamination. In future works, these avenues may prove rather useful for more complex applications beyond simple one-way sensor transduction—though this is itself still a highly demanded application. In addition, the guiding model provided by this work may be expanded and its resolution tuned below 0.5 pH, especially so with the support of surface instability simulations. Given the novelty of this phenomena's application, the technology is in its infancy; thus, with such promising potential ahead—and an ever-present need for such sensors and actuators in the hands of the every man, anywhere—there are many avenues to work along moving forward.

4. Experimental Section

Materials: Acrylamide (98.5%), acrylic acid, and Irgacure 2959 (2-Hydroxy-4′-(2-hydroxyethoxy)-2-methylpropiophenone) were all purchased from Fisher Scientific. *N,N′*-methylenebis(acrylamide) (Bis, 99%), 3-(trimethoxysilyl) propyl methacrylate, and urease from Canavalia Ensiformis Type III (20KU) were purchased from Sigma-Aldrich. Urea was purchased from Acros Organics. To induce environments of different pH, 0.5 M buffer solutions comprising anhydrous sodium phosphates (mono-, di-, and tri-basic) (Fisher Scientific) were utilized for alkaline environments (pH: 6.5–13), whereas a citric acid (anhydrous, Sigma-Aldrich)—sodium phosphate system was used for acidic environments (pH: 2–6).

Functionalization of Glass Slides for Gel Adherence: After cutting the glass slides to the appropriate size (roughly 1 in^2), the substrates were sonicated in three batches within ethanol, acetone, and water, respectively, for 15 min each. After thoroughly drying with N_2 gas, the rack of substrates was then placed in an ionization chamber and exposed to O_2 plasma on high power for 3 min, utilizing a Harrick Plasma PDC-001 plasma cleaner (115 V). Upon removal from the chamber, the rack of substrates was then quickly submerged in a solution of ethanol (600 mL), 10% acetic acid (18 mL), and 3-(trimethoxysilyl) propyl methacrylate (6 mL) for 48 h. The now functionalized substrates were stored in a sealed desiccator until their use.

Characterization: Swelling ratios were measured utilizing Canon photo camera in combination with a video analysis and modeling tool (Tracker). Elastic moduli were measured using the Dynamic Mechanical Analyzer (DMA) 850 from TA Instruments. Transmission curves were acquired with a Shimadzu UV-3101-PC UV—vis—NIR scanning spectrophotometer. The composition of samples was characterized by Thermo Nicolet NEXUS 670 FTIR.

Synthesis of Anionic Gel: Acrylamide, corresponding crosslinker Bis, and photoinitiator Irgacure were weighed out and added to a vial containing DI water, before mixing in acrylic acid into the solution via a syringe. In addition, though the ratio between the two polymers (acrylamide and acrylic acid) varied as the gel was tuned, the sum of the two never exceeded 20% of the solution by weight, though it dipped to as low as 8% (4% acrylamide and 4% acrylic acid). Meanwhile, Bis and Irgacure always remained in solution at 1% by weight. To make the pH-sensitive gel responsive to urea, varying amounts of urease were dissolved in the solution on a range from 0.1% to 1% by weight, with respect to the total solution. The proportion of deionized water in the system was adjusted accordingly across each recipe. Having fully homogenized the solution via stir rod for 15 min, ≈160 microliters of solution (160 μL) were then dropped into a square PDMS mold having a depth of 140 micrometers and a functionalized glass slide was slid overtop the solution, careful not to introduce air pockets. Once secure, the sample was placed on a cooling stage before placing the whole system in a UV oven and exposing the sample to 400 W of UV light for 60 s in a Dymax 2000-EC Series UV-curing flood lamp. Though not necessary to produce a functional pH-sensitive gel, the introduction of temperature sensitive enzymes like urease dictated that the sample temperature be kept low (in this case below 45 °C) to avoid denaturing of the enzyme within the hot environment produced by the UV lamp. Thus, the cooling stage was utilized in the synthesis of all gel recipes, both those containing urease and those that did not. Now polymerized and adhered to the glass slide, the sample was removed from the mold and ready for use, as shown in Figure 1a.

Supporting Information

Supporting Information is available from the Wiley Online Library or from the author.

Conflict of Interest

The authors declare no conflict of interest.

Author Contributions

I.F. and M.H. contributed equally to this work. X.H. and M.H. conceived the concept. X.H. supervised the project. I.F. conducted the experiments

and analyzed results. M.H. helped with the result analysis. I.F. wrote the initial draft. All authors contributed to the discussion of the manuscript.

Data Availability Statement

The data that support the findings of this study are available from the corresponding author upon reasonable request.

Keywords

buckling, hydrogels, scattering, sensors, surface instability, wrinkled

Received: February 26, 2021
Revised: March 26, 2021
Published online:

[1] S. Byrne, S. Seguinot-Medina, P. Miller, V. Waghiyi, F. A. von Hippel, C. L. Buck, D. O. Carpenter, *Environ. Pollut.* **2017**, *231*, 387.
[2] E. Kumarasamy, I. M. Manning, L. B. Collins, O. Coronell, F. A. Leibfarth, *ACS Cent. Sci.* **2020**, *6*, 487.
[3] P. C. Ray, H. Yu, P. P. Fu, *J. Environ. Sci. Heal. – Part C Environ. Carcinog. Ecotoxicol. Rev.* **2011**, *29*, 52.
[4] H. Ezoji, M. Rahimnejad, G. Najafpour-Darzi, *Ecotoxicol. Environ. Saf.* **2020**, *190*, 110088.
[5] C. Huffman, L. Ericson, *Assessment of Portable HAZMAT Sensors for First Responders*, https://www.ojp.gov/pdffiles1/nij/grants/246708.pdf **2012**.
[6] L. R. Molnar, J. V. Odom, B. G. DeRoos, C. J. Kolanko, in *Sensors and Command, Control, Communications, and Intelligence (C3I) Technologies for Homeland Security and Homeland Defense III*, Orlando, FL, USA **2004**, p. 60.
[7] N. Wilson, M. Kariisa, P. Seth, H. Smith, N. L. Davis, *MMWR. Morb. Mortal. Wkly. Rep.* **2020**, *69*, 290.
[8] L. Scholl, P. Seth, M. Kariisa, N. Wilson, G. Baldwin, *MMWR. Morb. Mortal. Wkly. Rep.* **2018**, *67*, 1419.
[9] S. A. Goodchild, L. J. Hubble, R. K. Mishra, Z. Li, K. Y. Goud, A. Barfidokht, R. Shah, K. S. Bagot, A. J. S. McIntosh, J. Wang, *Anal. Chem.* **2019**, *91*, 3747.
[10] M. Bentley, M. Bentley, *Syria and the Chemical Weapons Taboo*, Powells, Chicago **2018**.
[11] C. M. Whitaker, E. E. Derouin, M. B. O'connor, C. K. Whitaker, J. A. Whitaker, J. J. Snyder, N. R. Kaufmann, A. N. Gilliard, A. K. Reitmayer, *J. Macromol. Sci. Part A* **2017**, *54*, 40.
[12] M. Mayer, A. J. Baeumner, *Chem. Rev.* **2019**, *119*, 7996.
[13] J. R. Sempionatto, I. Jeerapan, S. Krishnan, J. Wang, *Anal. Chem.* **2019**, *912*, 378.
[14] A. J. Bandodkar, I. Jeerapan, J. Wang, *ACS Sensors* **2016**, *1*, 464.
[15] L. Ionov, *Mater. Today* **2014**, *17*, 494.
[16] M. Li, X. Wang, B. Dong, M. Sitti, *Nat. Commun.* **2020**, *11*, 3988.
[17] H. Banerjee, M. Suhail, H. Ren, *Biomimetics* **2018**, *3*, 15.
[18] Q. Shi, H. Liu, D. Tang, Y. Li, X. Li, F. Xu, *NPG Asia Mater.* **2019**, *11*, 64.
[19] S. Chatterjee, P. Chi-leung Hui, *Hydrogels – Smart Mater. Biomed. Appl.* **2019**, *13*.
[20] M. C. Koetting, J. T. Peters, S. D. Steichen, N. A. Peppas, *Mater. Sci. Eng. R Rep.* **2015**, *93*, 1.
[21] C. Echeverria, S. Fernandes, M. Godinho, J. Borges, P. Soares, *Gels* **2018**, *4*, 54.
[22] P. J. Flory, in *Principles of Polymer Chemistry*, **1953**.
[23] Dhanjai, A. Sinha, P. K. Kalambate, S. M. Mugo, P. Kamau, J. Chen, R. Jain, *TrAC Trends Anal. Chem.* **2019**, *118*, 488.
[24] C. Xu, G. T. Stiubianu, A. A. Gorodetsky, *Science (80-.)* **2018**, *359*, 1495.
[25] T. J. Dale, J. Rebek, *J. Am. Chem. Soc.* **2006**, *128*, 4500.
[26] J. Choi, M. Hua, S. Y. Lee, W. Jo, C. Y. Lo, S. H. Kim, H. T. Kim, X. He, *Adv. Opt. Mater.* **2020**, *8*, 1.
[27] M. Qin, M. Sun, R. Bai, Y. Mao, X. Qian, D. Sikka, Y. Zhao, H. J. Qi, Z. Suo, X. He, *Adv. Mater.* **2018**, *30*, 1.
[28] M. Sun, R. Bai, X. Yang, J. Song, M. Qin, Z. Suo, X. He, *Adv. Mater.* **2018**, *30*, 1804916.
[29] M. Qin, M. Sun, M. Hua, X. He, *Curr. Opin. Solid State Mater. Sci.* **2019**, *23*, 13.
[30] L. Phan, R. Kautz, E. M. Leung, K. L. Naughton, Y. Van Dyke, A. A. Gorodetsky, *Chem. Mater.* **2016**, *28*, 6804.
[31] F. Weiss, S. Cai, Y. Hu, M. Kyoo Kang, R. Huang, Z. Suo, *J. Appl. Phys.* **2013**, *114*, 073507.
[32] Q. Wang, X. Zhao, *Sci. Rep.* **2015**, *5*, 1.
[33] H. Davson, *The Eye*, Academic Press, New York **1962**.
[34] K. S. Gibson, E. P. T. Tyndall, *Visibility of Radiant Energy*, G.P.O., Washington, DC **1923**.
[35] W. S. Stiles, J. M. Burch, *Opt. Acta Int. J. Opt.* **1959**, *6*, 1.
[36] J. Cohen, G. Wyszecki, W. S. Stiles, *Color Science: Concepts and Methods, Quantitative Data and Formulas*, John Wiley & Sons, New York/Chichester **1968**.
[37] R. G. Keuhni, R. Ramanath, *Color Res. Appl.* **2004**, *29*, 183.
[38] A. J. Bartholomew, E. M. Lad, D. Cao, M. Bach, E. T. Cirulli, *PLoS One* **2016**, *11*, https://doi.org/10.1371/journal.pone.0148192.
[39] B. P. Schmidt, R. Sabesan, W. S. Tuten, J. Neitz, A. Roorda, *Sci. Rep.* **2018**, *8*, 8561.
[40] I. N. Bubanja, T. Bánsági, A. F. Taylor, *React. Kinet. Mech. Catal.* **2018**, *123*, 177.
[41] C. Eggenstein, M. Borchardt, C. Diekmann, B. Gründig, C. Dumschat, K. Cammann, M. Knoll, F. Spener, *Biosens. Bioelectron.* **1999**, *14*, 33.
[42] E. Loeser, M. Delacruz, V. Madappalli, *J. Chem. Eng. Data* **2011**, *56*, 2909.